

## 5C.5 EFFECT OF ENVIRONMENTAL MOISTURE ON RAINBANDS IN HURRICANES KATRINA AND RITA (2005)

Derek Ortt\* and Shuyi S. Chen  
University of Miami, RSMAS, Miami, FL

### 1. INTRODUCTION

Intense tropical cyclones (TC) often form secondary eyewalls and undergo eyewall replacement cycles (e.g. Willoughby et al., 1982). Studies using dry dynamical models concluded that secondary eyewalls were due to TC internal dynamics (e.g. Montgomery and Kallenbach, 1997; Kossin et al., 2000). Other studies found that eyewall replacement may be influenced by the large scale environment (e.g. Nong and Emanuel, 2003; Lonfat, 2004). The studies found that increased water vapor enhances TC rainbands, making secondary eyewall formation more likely.

A goal of the Hurricane Rainband and Intensity Experiment (RAINEX) was to address the cause of secondary eyewall formation (Houze et al., 2006, Chen 2006). RAINEX simultaneously sampled the environment and inner-core of Hurricanes Katrina, and Rita, two category 5 hurricanes in the Gulf of Mexico in 2005. This differed from previous field campaigns (e.g. Willoughby et al., 1982; Samsury and Zisper, 1995), which only investigated one region of the TC at any given time. RAINEX also had real-time, high resolution model forecasts for mission planning and post analysis.

This study uses the RAINEX data and model forecasts to evaluate the characteristics of the environment and rainbands in two major hurricanes. Rita underwent an eyewall replacement on September 22 while Katrina did not from the afternoon of August 27 until landfall. Ortt and Chen (2006) hypothesized that dry air surrounding Rita confined the rainbands into a pattern that favored secondary eyewall formation. The goal of this study is to demonstrate a physical mechanism through which water vapor affects rainband structure and secondary eyewall formation.

### 2. DATA AND MODEL

RAINEX observations and high resolution model output were used in this study. The observations include in situ aircraft measurements and microwave tropical rainfall measuring mission (TRMM) tropical

microwave imager (TMI) satellite data. The modeling component uses model output from the 5<sup>th</sup> generation mesoscale model from the Pennsylvania State University (MM5). Data for Katrina is analyzed from the afternoon of August 27 until 0000 UTC August 29 for Katrina and for September 21-22 for Rita. The results presented here are applicable to TCs over the open ocean and under low shear conditions.

Both TMI rainfall and total precipitable water (TPW) data were used. The TMI rainfall data has a 5km resolution and is used to evaluate the rainband structures. The TMI TPW data has a resolution of .25 degree and is used to evaluate the water vapor content in the outer environment, defined as 250-600km from the center.

The in-situ aircraft observations include flight level and dropsonde data from the NOAA and Naval Research Laboratory P3 and Air Force C-130 aircraft. The GPS dropsonde data from the P3 aircraft was used to determine how the water vapor content varied with height between the rainbands, while the G-IV dropsondes was used for the outer environment. All dropsondes have a temporal resolution of .5 seconds (Franklin et al., 2003). Data was interpolated onto a 25m (100m) vertical resolution from the surface to 2.5 km (11km) for the P3 (G-IV) dropsondes. The number of dropsondes used for each day from the P3 and G-IV is provided in Table 1.

Date	Number of Dropsondes (P3)	Number of Dropsondes (G-IV)
August 27 (Katrina)	27	20
August 28 (Katrina)	25	21
September 21 (Rita)	34	21
September 22 (Rita)	9	22

Table 1: Number of P3 and G-IV dropsondes used for Hurricanes Katrina (August 27 and 28) and Rita (September 21 and 22)

\*Corresponding author address: 4600 Rickenbacker Causeway, Miami FL 33143. E-mail: [dortt@rsmas.miami.edu](mailto:dortt@rsmas.miami.edu)

The flight level wind data is used to verify the existence, or lack of a secondary wind maximum. The flight level data has a temporal resolution of 30 seconds. Only legs through the TC center are used.

The MM5 output used in the study were real time forecasts of Katrina initialized at 0000 UTC, August 27 and Rita, initialized at 0000 UTC September 20. The Katrina forecast used GFDL (Kurihara et al., 1995) initial conditions and forecast fields as the boundary conditions. The Rita forecast used NOGAPS conditions (Rhome, 2007). These forecasts were the best of a mini ensemble. The forecasts featured 3 domains with resolutions of 15, 5, and 1.67km. The outer domain remained fixed and covered the entire Gulf of Mexico, the NW Caribbean, subtropical western Atlantic, and the eastern and central United States. The inner two domains used a nested vortex following technique developed by Chen and Tenerelli (2007).

### 3. RESULTS

#### 3.1. 3D Water Vapor Distributions

Hurricane Katrina and Rita were located in two different environments in terms of the amount of water vapor present. This is demonstrated in Fig. 1, which shows TMI TPW maps of Hurricanes Katrina and Rita from 2048 UTC August 27 and 0806 UTC September 22, 2005. Both hurricanes had TPW values exceeding 60 mm in the inner-core. However, the environmental TPW was different. Hurricane Katrina was located in an environment with a mean TPW > 56 mm. Hurricane Rita was located within an environment with a mean TPW between 51-54mm within the outer environment, as defined as 250-600km from the center. The results shown in Fig. 1 were not isolated to the times of the TMI passes. Instead, the differences between the two TCs were consistent while each storm was in the Gulf of Mexico.

While the TMI TPW showed a large difference in the amount of water vapor in the environments of the two storms, it did not provide any information as the variability with height. Therefore, we used GPS dropsondes from the P3 and G-IV aircraft. Figure 2 shows the composite daily mean vertical RH profiles from the G-IV and P3 aircraft from the outer environment and between the rainbands, respectively.

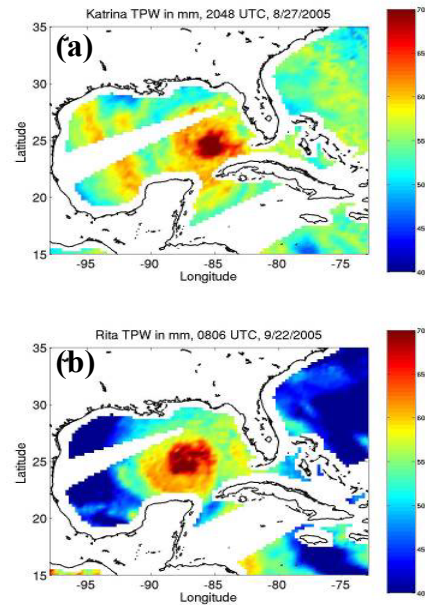


Figure 1: TMI TPW of Hurricanes Katrina (a) from 2048 August 27 and Rita (b) from 0806 September 22. Blue represents areas of low TPW and reds represent areas of high TPW.

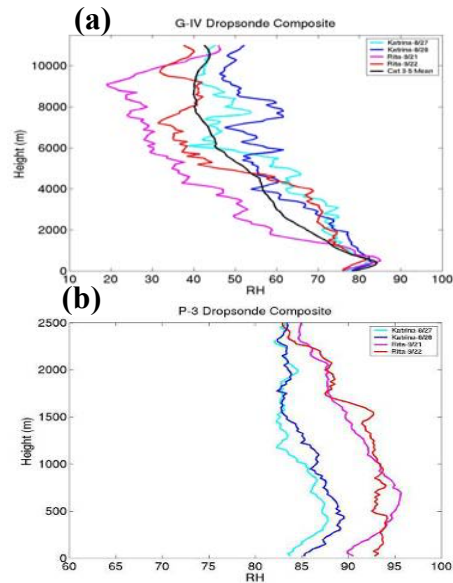


Figure 2: Observed environmental (a) and rainband (b) composite mean RH vertical profiles from Katrina on August 27 (cyan) and 28 (blue) and Rita from September 21 (magenta) and 22 (red). In (a), black denotes the 1998-2005 composite mean environmental category 3-5 hurricane vertical RH profile from Ortt (2007).

The dropsonde data show that the differences in environmental water vapor are in the middle troposphere. Composite mean environmental RH values

are 10-20 percent higher in Katrina than Rita in the middle troposphere. In addition, the environment has anomalously high RH in Katrina when compared with the category 3-5 hurricane composite mean profile between 5-8km. The environment that Rita was in had anomalously low RH between 5 and 8km. (Ortt, 2007). Between the rainbands, however, Rita has composite RH values of 5-10 percent greater than those from Katrina. This indicates the presence of a strong radial moisture gradient in Rita with a much weaker gradient in Katrina.

The MM5 forecasts reproduced the observed moisture gradient. Figure 3 shows the MM5 daily environmental and rainband composite RH profiles for the two storms. While the absolute RH values are somewhat higher for both the rainbands and environment, especially within the boundary layer, the differences between Katrina and Rita are present. Composite RH values in the outer environment of Katrina were about 15 percent greater than for Rita between 5-8km. Between the rainbands, RH values were 3-5 greater in Rita than in Katrina.

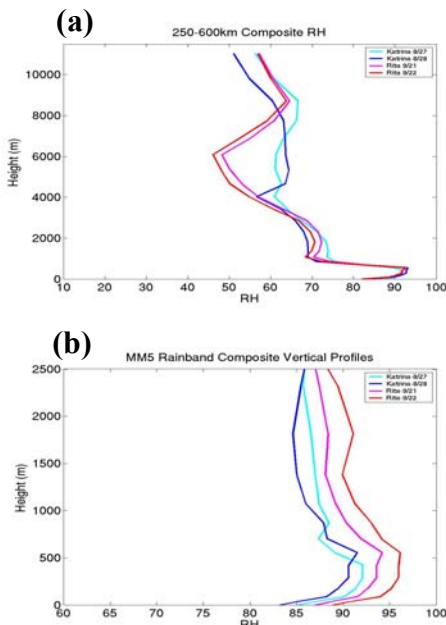


Figure 3: MM5 environmental (a) and rainband (b) composite mean RH vertical profiles from Katrina on August 27 (cyan) and 28 (blue) and Rita from September 21 (magenta) and 22 (red).

### 3.3 Rainband Structures

To quantify the rainband structures, a rainband circularity index was created. This index measures how much a convective rainband extends around the storm at any given radius. The index is defined as

$$C(i) = rr_{>12.5}(i) / rr(i) \quad (1)$$

where  $C$  is the rainband circularity,  $rr_{>12.5}$  is the number of grid points with rainrate greater than  $12.5 \text{ mm h}^{-1}$ ,  $rr$  is the total number of grid points, while  $i$  denotes each successive 5km radius. Any rainbands with a  $C > .5$  are considered possible eyewalls or secondary eyewalls, consistent with current National Hurricane Center practice (Williamson et al., 2007). The rainbands with  $C > .5$  are then confirmed as eyewalls if there is a wind maximum, consistent with Willoughby et al. (1982).

Figure 4 shows the TMI rainrate and rainband circularity of Katrina from 2135 UTC August 28. A rainband with circularity near .9 is associated with the eyewall. Rainband circularity is less than .25 for all other rainbands within 200km of the center. This indicates that there is not a secondary eyewall present at this time.

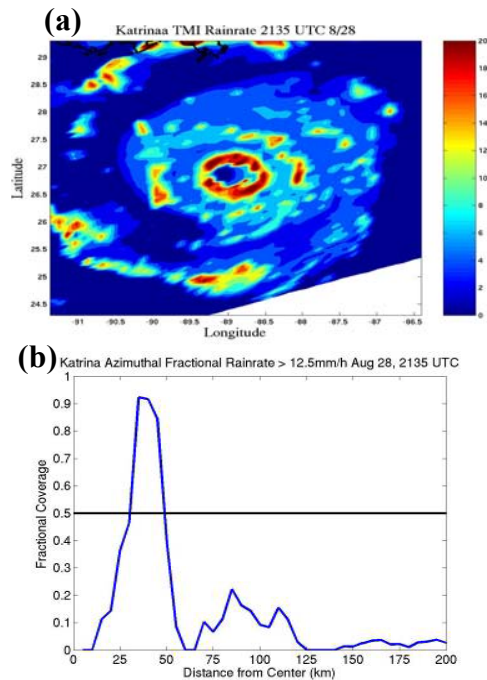


Figure 4: TRMM TMI rain rate (mm/h) of Katrina (a) and rainband circularity (b) from 2130 UTC August 28, 2005. Black line represents secondary eyewall candidate threshold of .50.

Rita, in contrast had rainbands with high circularity. Figure 5 shows the TMI rainrate and rainband circularity of Rita from 0812 UTC, September 22. At this time, there were multiple rainbands with circularity  $> .5$  outside of the eyewall. This indicates that there may have been a secondary eyewall present. The flight level wind data (Fig. 6) confirms the existence of a secondary eyewall. A well-defined wind maximum with winds approximately the same value of those of the eyewall was present on September 22. The flight level winds confirm there was no secondary eyewall in Katrina.

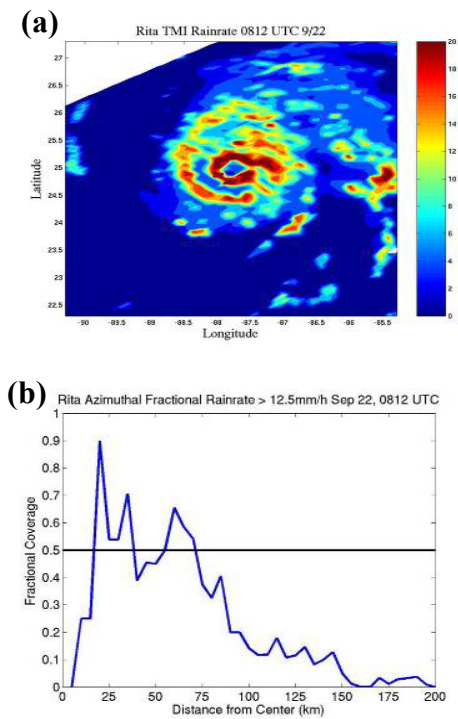


Figure 5: TRMM TMI rain rate (mm/h) of Rita (a) and rainband circularity (b) from 0806 UTC September 22, 2005. Black line represents secondary eyewall candidate threshold of .50.

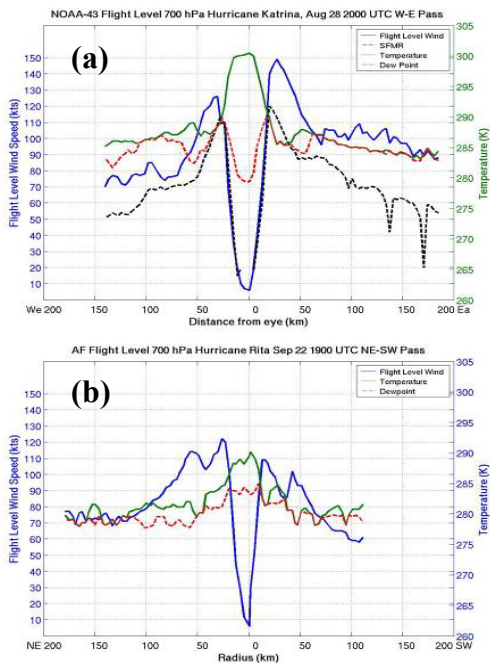


Figure 6: NOAA 43 flight level data for Hurricane Katrina at 2100 UTC, August 28 (a) and Air Force flight level data for Rita from 1900 UTC Sept 22 (b). Blue represents flight level wind, dashed black: SFMR surface wind, green: temperature, and blue: dewpoint.

The rainband structures in the MM5 were similar to the observations. Figure 7 shows a time-radius diagram of the rainband circularity of the two hurricanes. Katrina maintained a single eyewall throughout the forecast period. Late on August 28, there were periods where there was rainband circularity greater than .5 outside of the eyewall. However, these rainbands were transient, lasting less than 3 hours. In contrast, Hurricane Rita underwent an eyewall replacement in the MM5. On September 21, a rainband developed at a radius of 100-150km. The rainband slowly wrapped its way around the storm and its circularity exceeded .5 early on September 22. Around 1200 UTC, the primary eyewall began to weaken as the outer eyewall contracted and its circularity increased to > .6. By 1800 UTC, the primary eyewall was dissipating and the outer eyewall established itself as the new eyewall.

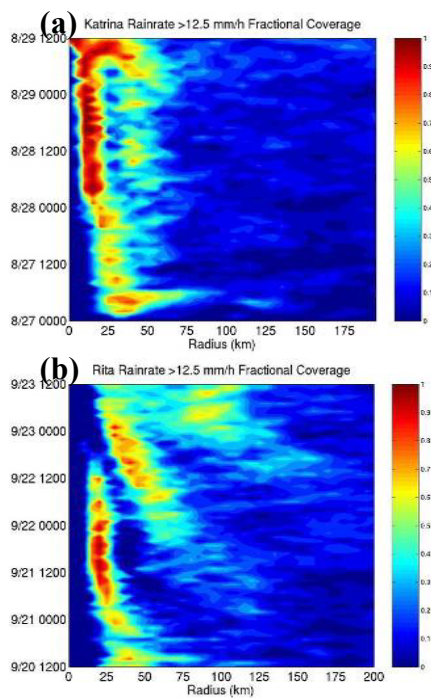


Figure 7: MM5 rainband circularity of Hurricane Katrina from 0000 UTC August 27 to 1200 UTC August 29 (a) and Rita from 1200 UTC September 20 to 1200 UTC September 23 (b). Blues denote low rainband circularity while yellows and reds denote high rainband circularity.

### 3.4 Moist Stability Index

The previous two sections have shown the differences in the water vapor distributions and rainband structures of Hurricanes Katrina and Rita. We now provide an explanation for how the environmental water vapor affected the rainbands.

The working hypothesis was that the Outer environment in Rita was stable, while the outer environment of Katrina was unstable. A stable environment would confine convective rainbands to the hurricane circulation while an unstable environment would allow a more spiraling pattern. We first tested this hypothesis by approximating the potential instability by evaluating the integral of  $\theta_{es} - \theta_e^*$ , where  $\theta_{es}$  is the surface equivalent potential temperature and  $\theta_e^*$  is the saturation equivalent potential temperature at all levels. The observations showed an unstable environment for Katrina and a stable environment for Rita. However, the potential instability from the MM5 was similar for the two storms. A likely reason was the MM5 boundary layer being too moist.

A measure of stability due to mid tropospheric moisture was required. Adapting common severe weather indices provided in Sturtevant (1995), we created a moist stability index (MSI) that measures the vertical temperature lapse rate and the amount of water vapor in the middle troposphere. The (MSI) is defined as

$$MSI = (T_{700} - 3T_{500} - T_{400}) + (TD_{700} + TD_{500} + TD_{00}) \quad (2)$$

where T is the temperature, TD is the dewpoint, and the subscripts denote the respective pressure level in hPa. The units of the index are K.

Figure 8 shows the observed and MM5 environmental MSI for Katrina and Rita. Both the observations and MM5 show Rita located in a relatively stable environment compared with Katrina. Observed MSI values for Katrina are more than 10K higher than Rita. In the MM5 the differences are somewhat less, though the trend is the same as the observed.

The rainband activity in the MM5 is well correlated with areas of high instability. This is shown in Fig. 9, which shows the evolution of the rainbands and instability. In both MM5 forecasts, the organized rainbands originated within the 10K MSI contour. This radius was  $>400\text{km}$  from the center in Katrina late on the 27<sup>th</sup> and early on the 28<sup>th</sup>. This allowed the rainbands to originate farther from the center, promoting a more spiraling pattern with lower circularity. In Rita, the 10K radius was within 300km of the center. The cyclonic circulation of the wind field

resulted in the rainbands having a high circularity. These rainbands then formed into a secondary eyewall.

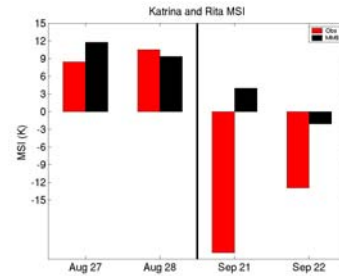


Figure 8: Observed (black) and MM5 (red) daily composite mean MSI of Hurricanes Katrina (left) and Rita (right) within the outer storm environment. Observed mean was derived from GPS dropsondes.

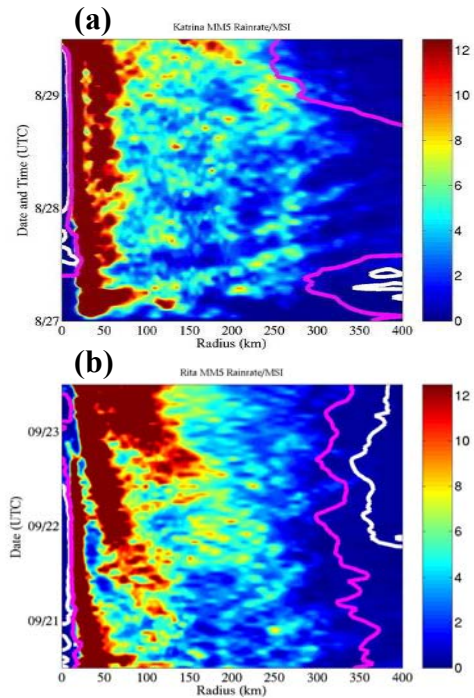


Figure 9: Azimuthally averaged MM5 rain rate ( $\text{m s}^{-1}$ , shaded) overlaid with 2.5K (white) and 10K (magenta) MSI contours of Hurricanes Katrina (a) and Rita (b). The times are the same as in Fig. 7.

## 4. SUMMARY AND DISCUSSION

Hurricanes Katrina and Rita were two category 5 hurricanes in the Gulf of Mexico in 2005 with very different rainband structures and environmental water vapor distributions. Hurricane Katrina was in a moist, unstable environment and had rainbands with low circularity that spiraled into the center. Rita was in a dry, stable environment and had rainbands with high

circularity that formed into a secondary eyewall. The rainband activity was well-correlated with the areas where the MSI was high. In Katrina, these areas were farther from the center. In Rita, the rainbands were confined to the main hurricane circulation. This forced the rainband circularity to increase, due to advection of the tangential wind. These results are summarized in Fig. 10, which is a conceptual model of how environmental water vapor affects the rainbands. In this model, a sharp horizontal moisture gradient confines the rainbands into a pattern similar to that of Rita. The rainbands in the sharp gradient case favor the formation of a secondary eyewall. As stated in Samsury and Zipser (1995), a rainband outside of the primary eyewall disrupts the moist surface inflow into the eyewall. The inflow that does reach the eyewall has lower  $\theta_e$  due to the convective downdrafts associated with the secondary eyewall (Powell, 1990). Additionally, the secondary circulation associated with the secondary eyewall causes subsidence to spread over the primary eyewall and was documented in Rita (Houze et al., 2007). These effects combine to cause the primary eyewall to weaken and eventually dissipate. With a weak moisture gradient, the rainbands spiral into the center from a greater radius and have less circularity. This pattern is not favorable for a secondary eyewall to form.



Figure 10: Conceptual model of moisture gradient and TC rainband structures. Relatively weak gradient (left) may favor for extended spiraling rainbands as in the case of Katrina, whereas a strong moisture gradient may be a factor that confining the rainbands at the radius where the strong gradient is. Areas inside of the red circle represent very moist and unstable environment while areas outside of the light blue represent dry and stable. The teal shapes represent the TC rainbands.

During the eyewall replacement cycle, Hurricane Rita weakened from a category 5 hurricane to a category 4 hurricane. These results indicate that environmental water vapor is able to affect intensity in a low-shear environment by affecting the rainband structures. Specifically, the environmental water vapor confined the rainbands into a pattern that promotes the formation of a secondary eyewall. This results in a temporary

weakening, which may then be followed by re-intensification, if environmental conditions are conducive for intensification.

### Acknowledgements

We would like to thank NOAA HRD for providing the dropsonde data from the NOAA P3 and G-IV aircraft, the NRL and NCAR for the NRL P3 data, Remote Sensing Systems for the TMI TPW data, and NASA for the TMI rainfall data. We also thank Dr. Wei Zhao and Mr. John Cangialosi for their assistance during the course of this study. We also would like to thank Mr. Falko Judt for thoughtful discussions during the study. This work was funded by NSF RAINEX grant ATM-0432717 and by AMS and University of Miami fellowships.

### References:

- Chen, S. S., 2006: Overview of RAINEX modeling of 2005 hurricanes. *The 27<sup>th</sup> Conf. on Hurricanes and Tropical Meteorology*. 23-27 April 2006, Monterey, CA, Amer. Meteor. Soc. **12A.2**.
- Chen, S. S., and J. E. Tenerelli, 2007: Simulation of hurricane lifecycle and inner-core structure using a vortex following mesh refinement: Sensitivity to model grid resolution. *Mon. Wea. Rev.*, in revision.
- Franklin, J. L., M. L. Black, and K. Valde, 2003: GPS dropwindsonde profiles in hurricanes and their operational implications. *Wea. and Forecasting* **18**, 32-44.
- Houze, R. A., S. S. Chen, and co-authors, 2006: The Hurricane Rainband and Intensity Change Experiment (RAINEX): Observations and modeling of Hurricanes Katrina, Ophelia, and Rita (2005). *Bull. Amer. Meteor. Soc.*, **87**, 1503-1521.
- Houze, R. A., S. S. Chen, and co-authors, 2007: Hurricane intensity and eyewall replacement. *Science*, **315**, 1235-1239.
- Kossin, J. P., W. H. Schubert, and M.T. Montgomery, 2000: Unstable interactions between a hurricane's primary eyewall and a secondary ring of enhanced vorticity. *J. Atmos. Sci.*, **57**, 3893-3917.
- Kurihara, Y., R. E. Tuleya, and R. J. Ross, 1995: Improvements in the GFDL hurricane prediction system. *Mon. Wea. Rev.*, **123**, 2791-2801.

Lonfat, M., 2004: Tropical cyclone rainfall: An observational and numerical study of the structure and governing physical mechanisms. PhD Dissertation, University of Miami, 66pp.

Montgomery, M. T. and R. J. Kallenbach, 1997: A theory for vortex Rossby waves and its application to spiral bands and intensity changes in hurricanes. *Q. J. R. Met. Soc.*, **123**, 435-465.

Nong, S. and K. Emanuel, 2003: A numerical study of the genesis of concentric eyewalls in hurricanes. *Q. J. R. Met. Soc.*, **129**, 3323-3338.

Ortt, D., and S. S. Chen, 2006: Rainbands and secondary eyewall formation as observed in RAINEX. <sup>th</sup> *27 Conf. on Hurricanes and Tropical Meteorology*. 23-27 April 2006, Monterey, CA, Amer. Meteor. Soc. **12A.5**.

Ortt, D., 2007: Effects of environmental water vapor on tropical cyclone structure and intensity. Master's Thesis, University of Miami 91pp.

Powell, M.D., 1990: Boundary layer structure and dynamics in outer rainbands. Part II: Downdraft modification and mixed layer recovery. *Mon. Wea. Rev.*, **118**, 918-938.

Samsury, C.E. and E. J. Zisper, 1995: Secondary wind maxima in hurricanes: Airflow and relationship to rainbands. *Mon. Wea. Rev.*, **123**, 3502-3517.

Sturtevant, John S., 1995. *The Severe Local Storm Forecasting Primer*, 197 pp.

Rhome, J. R., 2007: Technical Summary of the National Hurricane Center Track and Intensity Models. Available at <http://www.nhc.noaa.gov/modelsummary.shtml>

Williamson S. P. and co-authors, 2007: National Hurricane Operations Plan. Available at <http://www.ofcm.gov/nhop/07/nhop07.pdf>.

Willoughby, H. E., J. A. Clos, and M. G. Shoreibah, 1982: Concentric eye walls, secondary wind maxima, and the evolution of the hurricane vortex. *J. Atmos. Sci.*, **39**, 395-411.